Global Mode Control and Stabilization for Disruption Avoidance in High-β NSTX Plasmas*

J.W. Berkery[1], S.A. Sabbagh[1], A. Balbaky[1], R.E. Bell[2], R. Betti[3], J.M. Bialek[1], A. Diallo[2], D.A. Gates[2], S.P. Gerhardt[2], O.N. Katsuro-Hopkins[1], B.P. LeBlanc[2], J. Manickam[2], J.E. Menard[2], Y.S. Park[1], M. Podestà[2], F. Poli[2], H. Yuh[4]

[1]Department of Applied Physics and Applied Mathematics, Columbia University, New York, NY, USA

[2]Princeton Plasma Physics Laboratory, Princeton University, Princeton, NJ, USA

[3]Laboratory for Laser Energetics, University of Rochester, Rochester, NY, USA

[4]Nova Photonics, Inc., Princeton, NJ, USA

E-mail contact of main author: jberkery@pppl.gov

Abstract. Global mode control and stabilization are studied to avoid disruptions in high-β NSTX plasmas. Dedicated experiments in NSTX using low frequency active MHD spectroscopy of applied, rotating n = 1 magnetic fields revealed key dependencies of stability on plasma parameters. Stability is weakest at intermediate, not the highest, values of β_N/l_i, in agreement with other NSTX active control experiments. Stable plasmas at high β_N appear to benefit from reduced collisionality, in agreement with expectation from kinetic resistive wall mode (RWM) stabilization theory. MHD spectroscopy measurements add additional support to the established theory of RWM stability through kinetic mode-particle resonances, showing reduced amplitude when the $E\times B$ and precession drift frequencies are in a range of resonance. Kinetic RWM stabilization theory shows that collisions have competing effects: they both dissipate the mode energy and damp the stabilizing kinetic effects. The low collisionality of future machines can improve RWM stability, but only if the plasma rotation is in a favorable resonance. Two active control techniques were tested to avoid disruption when profile transients cause instability. Disruption probability was reduced from 48% to 14% in high β_N/l_i plasmas with dual field component (radial and poloidal) active control. Time domain analysis with the VALEN code reproduces the dynamics of the mode amplitude as a function of feedback phase and determines the optimal gain. A model-based RWM state space controller sustained long-pulse, high-β_N discharges. Plasmas limited only by coil heating constraints have exceeded β_N = 6.4, β_N/l_i = 13. Application of the kinetic stability model to ITER plasmas indicates that alpha particles are normally required for RWM stability, but internal transport barriers may be beneficial to stability by lowering the $E\times B$ frequency.

1. Introduction

Global MHD instabilities in tokamaks (such as the resistive wall mode (RWM)) are critically important to avoid or control as they lead to plasma disruption, terminating the discharge and leading to large, potentially damaging electromagnetic forces and heat loads on the structure of magnetic fusion producing devices. Plasma operation below marginal stability points (that depend on, for example, plasma beta, internal inductance, rotation profile) is insufficient to ensure disruption-free, continuous operation in tokamaks, including ITER inductive or advanced scenarios because of excursions from these conditions due to transients in plasma profiles. Such transients can rapidly change a stable operational point to an unstable plasma state. In addition, recent research has found that marginal stability conditions are not simply monotonic functions of important plasma parameters, such as rotation profile [1]. Therefore, understanding plasma stability gradients vs. key profiles is essential for all operational states in devices such as ITER, or a Fusion Nuclear Science Facility (FNSF) [2]. The National

* Supported by US DOE Contracts DE-FG02-99ER54524, DE-AC02-09CH11466, and DE-FG02-93ER54215

Spherical Torus Experiment (NSTX) has previously investigated passive stabilization [3] and demonstrated active control [4] of RWMs, accessing high normalized beta, β_N = 7.4 ($\beta_N \equiv 10^8 \langle\beta_t\rangle aB_0/I_p$, ($\beta_t \equiv 2\mu_0\langle p\rangle/B_0^2$), where $\langle p\rangle$ is the volume-average plasma pressure, B_0 is the magnetic field on axis, a is the minor radius, and I_p is the plasma current) [5]. Current research focuses on greater understanding of the stabilization physics, projection to future devices, quantitative comparison to experiment, and demonstration of improved active control techniques that can reduce resonant field amplification (RFA) or disruptions due to profile transients causing instability.

2. High β_N operation and disruptions

Next-step STs and steady-state advanced tokamaks both aim to operate continuously at high β_N and high non-inductive current fraction. High bootstrap current fraction yields a broad current profile, equating to low plasma internal inductance, l_i. This is favourable for efficient non-inductive operation, but is generally unfavourable for global MHD mode stability, reducing the ideal toroidal mode number n = 1 no-wall beta limit, $\beta_N^{no\text{-}wall}$. Past high β_N operation with l_i typically in the range 0.6 < l_i < 0.8 has an n = 1 $\beta_N^{no\text{-}wall}$ computed by the DCON code to be 4.2 – 4.4 [6]. Operation at β_N > 6.5 and β_N/l_i > 13.5 has been demonstrated transiently, with pulse-averaged β_N (averaged over constant plasma current), $\langle\beta_N\rangle_{pulse}$ > 5.5 in low l_i plasmas in the range 0.4 < l_i < 0.6 with active n =1 mode control (Fig. 1). Pulse-averaged values of (l_i, β_N) now intercept the planned operational ranges for ST-CTF [2] and ST Pilot plants [7]. Especially important is that the ideal n = 1 no-wall stability limit is significantly reduced at these low l_i values, so that β_N now exceeds the DCON computed $\beta_N^{no\text{-}wall}$ for equilibrium reconstructions of these plasmas by up to a factor of two. In addition, synthetic variations of the pressure profile for plasmas with l_i ~ 0.38 show these equilibria to be at the purely current-driven ideal kink stability limit, as they are computed to be ideal unstable at all values of β_N. In this operational regime, passive or active kink and resistive wall mode (RWM) stabilization is therefore critical. The disruption probability due to unstable RWMs was reduced from 48% in initial low l_i experiments to 14% with dual field component control (Sec. 5). Remarkably, the reduced disruption probability was observed mostly in plasmas at high β_N/l_i > 11; disruptions occurred more frequently at intermediate values of β_N/l_i as shown in Fig. 1.

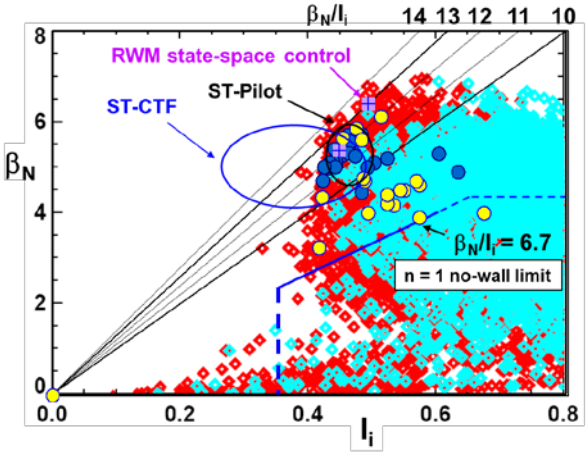

FIG. 1. High β_N, low l_i operational space in NSTX. Red/cyan points indicate plasmas with/without n=1 active RWM control. Blue circles indicate stable long pulse plasmas with active RWM control; yellow indicates disruptions.

3. Active MHD spectroscopy analysis and RWM stability vs. plasma parameters

Dedicated experiments were performed in NSTX to determine the stability of stable, long pulse, high β_N plasmas as a function of key plasma parameters for kinetic RWM stability (such as plasma rotation profile and ion collisionality), using MHD spectroscopy. This is a natural extension of past experiments that directly accessed the RWM marginal stability point and found quantitative agreement to kinetic RWM stability theory [1,5]. An important difference from joint experiments on DIII-D [8,9] is that here the MHD spectroscopy is being performed on plasmas that access marginal stability, with a small portion of these plasmas

becoming unstable. In these cases, RFA amplitude grows rapidly (on the RWM instability growth time) and significantly.

Active MHD spectroscopy is an experimental diagnostic technique that is used as a measure of kink-ballooning/RWM mode stability when the modes are stable [10]. The "low-frequency" version of this technique typically measures the amplification and phase shift of a traveling n = 1 applied tracer field. Experimental evidence to date has shown increasing amplitude and phase shifts to indicate decreasing mode stability [10]. Here, a 40 Hz co-NBI rotating n = 1 seed field was applied with the NSTX RWM coils, and the RFA of that applied field was measured using magnetic sensors. MHD spectroscopy analysis software was upgraded to match the analysis in Ref. [10] for more direct comparison to results in the literature.

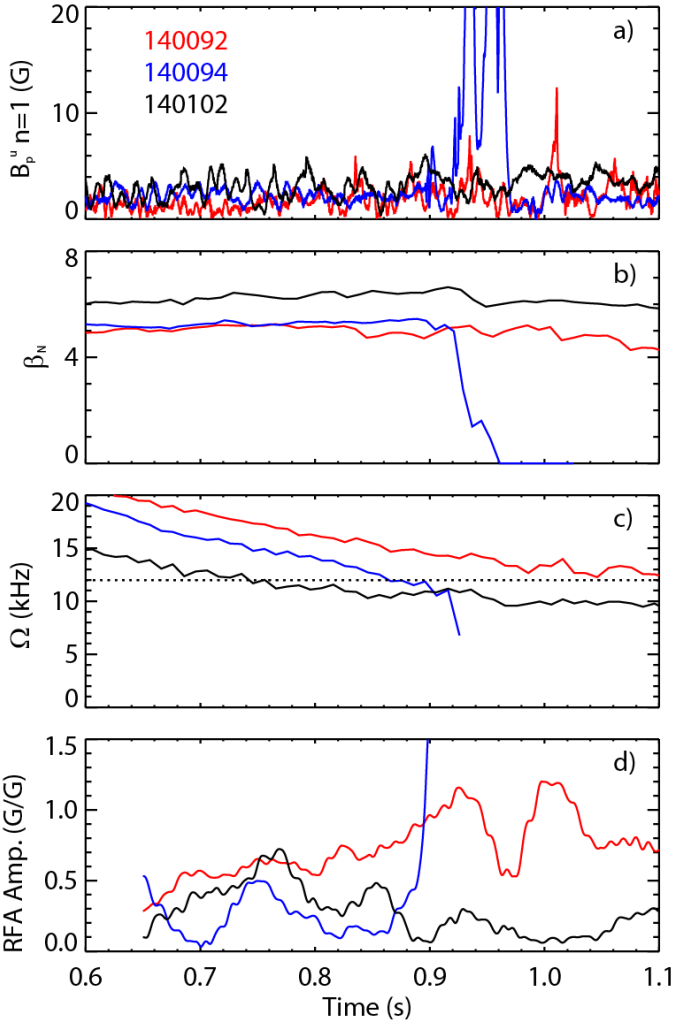

FIG. 2. Comparison of multiple NSTX discharges showing, a) n=1 signal on the upper poloidal magnetic field sensors, b) β_N, c) carbon toroidal rotation near the core (CHERS channel 6)), d) n = 1 RFA amplitude, vs. time.

Figure 2 shows a comparison of three of the many NSTX discharges from this experiment, showing the decomposed n = 1 perturbation amplitude on the upper poloidal magnetic field sensors, β_N, carbon toroidal rotation at the plasma core (CHERS channel 6), and n = 1 RFA amplitude, vs. time. Each discharge was subject to varying levels of non-resonant n = 3 magnetic braking [11], which provided controlled, steadily decreasing rotation to low rotation levels. The discharge shown by the blue trace goes unstable at 0.9 s when the rotation reached ~12 kHz. The discharge shown in red has the same β_N, but higher rotation and maintains stability, as might be expected from early RWM stabilization theory. However, twice this discharge approaches marginal stability, at ~13-14 kHz, near the rotation level that drives the discharge shown in blue unstable, but does not go unstable (see (a) and (d)). The discharge shown in black has *higher* β_N and *lower* rotation, but maintains stability and has low RFA, which is counter-intuitive based on stability models yielding a simple critical rotation velocity for stability. Resonant kinetic RWM stabilization physics allows such behavior at low rotation [1]. Note that the RFA level for this discharge also peaks near the same rotation level at which the discharge shown in blue becomes unstable.

The result of greater disruption probability at intermediate values of β_N/l_i (shown in Sec. 2) agrees with active MHD spectroscopy diagnosis, used to determine the proximity to marginal stability. The RFA amplitude taken from the full database of twenty discharges, during time periods without rotating or locked tearing modes, shows an increase to a broad peak near β_N/l_i = 10 (Fig. 3). There is a large variation in RFA amplitude at a given β_N/l_i because other

parameters, chiefly plasma rotation, are not constant. RFA amplitude then decreases at higher values of β_N/l_i, indicating increased mode stability. This positive result is presently not thought to be a second stability region for the RWM, but is related to proximity to broad resonances in plasma rotation providing kinetic stabilization of the RWM [1,5], as will be shown in the next section.

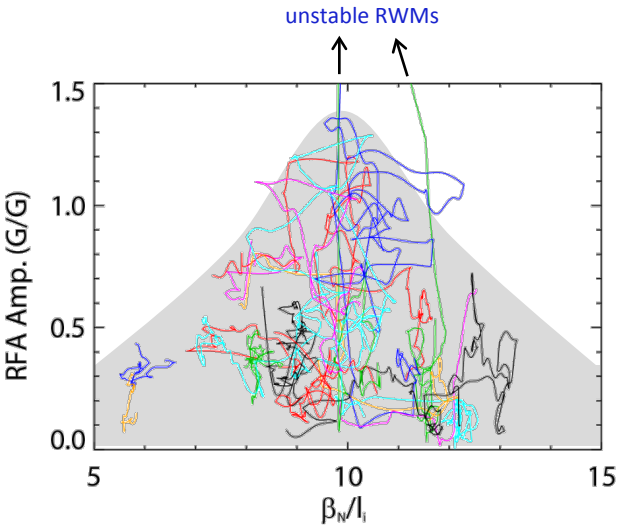

FIG. 3. RFA amplitude vs. β_N/l_i, showing generally decreasing stability as β_N/l_i is increased toward ~10.

Theoretical expectation is that collisions can have the competing effects of both dissipating mode energy and damping stabilizing kinetic effects [12]. Plasmas which have a favorable rotation profile providing a stabilizing resonance with ion motion can benefit from a reduction in collisionality, which allows those resonant effects to be stronger (Fig. 4) [12]. Figure 5 shows the trajectory of the RFA amplitude over the discharge for the database of 20 NSTX shots, over which an average ion-ion momentum-transferring collision frequency, ν_{ii}, is varied experimentally by a factor of 3.75. The theoretically expected gradients in kinetic RWM stability are generally reproduced by the upper/lower boundaries of the n = 1 RFA amplitude. At high RFA amplitude (the upper boundary), the plasma is off-resonance, and there is almost no change in RWM stability (indicated by the n = 1 RFA amplitude) vs. ν_{ii}. At low n = 1 RFA amplitude (the lower boundary), the plasma has greater stabilization by kinetic resonances, and there is a clear increase in RWM stability (decrease in RFA amplitude) as ν_{ii} is reduced. Here, ν_{ii} is averaged over $0.55 < \psi/\psi_a < 0.75$ of the profile, inside of the pedestal. At low collisionality, the plasma stability gradient is expected to increase as a function of rotation (Fig. 4) [12]. This emphasizes the utility and need for rotation and RWM control in lower collisionality devices. Active feedback is needed when either slow, controlled or sudden, uncontrolled changes take the plasma through a marginal stability point. Such active control will be

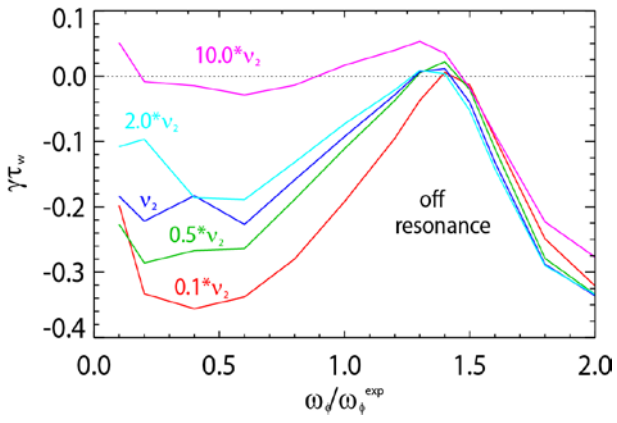

FIG. 4. (Reproduced from Ref. [12]): $\gamma\tau_w$ vs. scaled experimental rotation $\omega_\varphi/\ \omega_\varphi^{exp}$ for NSTX shot 140132 at 0.704s at various levels of scaled collisionality.

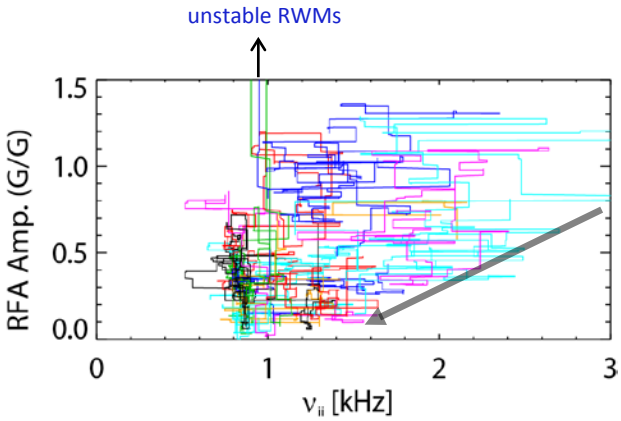

FIG. 5. RFA amplitude vs. an average ion-ion collision frequency, showing generally increasing stability as collisionality is decreased, especially at lower RFA levels (more stable plasmas).

discussed in Sec. 5.

4. Connection between RFA analysis and kinetic RWM stability physics theory

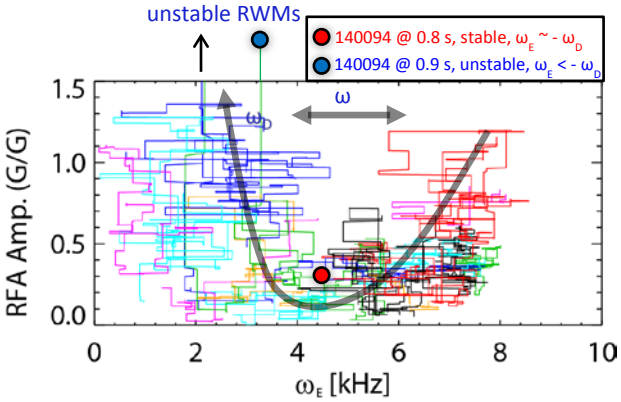

FIG. 6. RFA amplitude vs. an average E×B frequency, ω_E.

Previous NSTX research and kinetic theory have established the present understanding that a single point rotation measurement (as shown in Fig. 2c) is not sufficient as an indicator of RWM stability. Full kinetic RWM calculations with the MISK code [13] capture the necessary physics, with an example shown below. An intermediary step that can provide physical insight, however, is to examine the effect of plasma rotation in the context of kinetic resonances between the mode and the particles by examining the $E\times B$ frequency, ω_E, and comparing to the ion precession drift frequency, ω_D. Figure 6 shows RFA amplitude plotted against an average ω_E, taken over $0.55 < \psi/\psi_a < 0.75$ of the profile. In Fig. 7 one can see that $-\omega_D$ for hot thermal ions in this ψ range averages roughly 4.5 kHz for discharge 140094 at time 0.8 s (also shown is $t = 0.9$ s, the time just before this discharge goes unstable in Fig. 2). Although the comparison is for higher energy particles than expected, we note that $\omega_E \sim -\omega_D$ at the stable time, and $\omega_E < -\omega_D$ at the unstable time, corresponding to the middle and left sides of Fig. 6, respectively. This can explain the low RFA amplitude in this ω_E range in Fig. 6, with low rotation instability below this, and intermediate rotation marginal stability above. Presumably the RFA would return to lower values at higher ω_E as the mode begins to resonate with the bounce frequency, but this higher level of rotation was not explored in this particular experiment. Similar experiments with MHD spectroscopy in stable plasmas in DIII-D yielded conclusions similarly supportive of kinetic stability theory [8].

This type of comparison is insightful, but neglects the more complex and complete physics that is included in the full MISK code [13] calculation of kinetic stabilizing effects. Figure 8 shows the MISK-calculated growth rate normalized to the wall eddy current decay time, $\gamma\tau_w$, vs. scaled experimental rotation profiles for the same two equilibria from discharge 140094, at 0.8 s (red) and 0.9 s (blue). The earlier time is predicted to be more stable, in agreement with the experiment (see Fig. 2). Also, MISK predicts instability at 0.9 s, albeit at a slightly

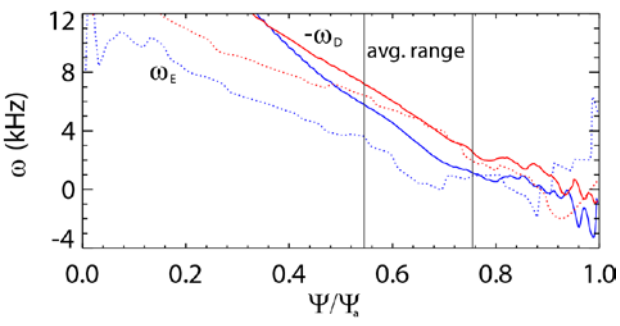

FIG. 7. E×B frequency, ω_E, profiles (dashed) and $-\omega_D$ profiles (for $\varepsilon/T = 2.5$ and zero pitch angle), vs. ψ/ψ_a, for NSTX discharge 140094 at 0.8 s (red) and 0.9 s (blue).

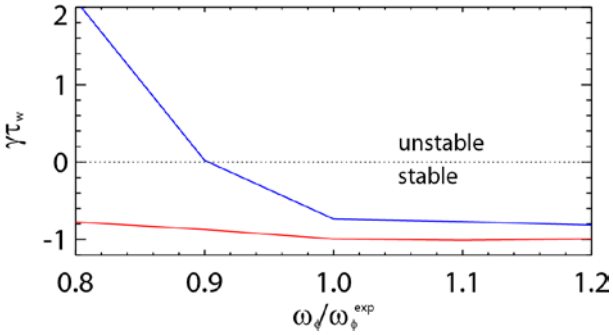

FIG. 8. MISK-calculated normalized growth rate, $\gamma\tau_w$, vs. scaled experimental rotation profiles for two equilibria from discharge 140094, at 0.8 s (red) and 0.9 s (blue).

(10%) lower rotation than the experimental reality. Note that these calculations were performed without energetic particles, which can be expected to add a stabilizing effect [2].

5. Dual-field component active RWM control and model-based RWM controllers

When passive stability proves insufficient, active feedback control of RWMs becomes necessary. Two approaches for improved RWM control have been used and studied. First, combined radial (24 B_r sensors) and poloidal (23 B_p sensors) field sensor feedback gain and phase were scanned in NSTX experiments to produce significantly reduced n = 1 field and improved stability. The previously mentioned (Fig. 1) reduction of disruption probability at high β_N/l_i was achieved with this dual field component control. The fast (2-3 ms) RWM growth was found to be controlled by B_p feedback, while B_r feedback controlled slower n = 1 RFA. Time domain analysis of active control with the VALEN code reproduces the mode dynamics as a function of feedback phase and determines the optimal gain. Modelled feedback evolution agrees with experiment for radial sensor variations examined (Fig. 9), and also shows the optimal gain is still a factor of 2.5 greater than the value used in experiments.

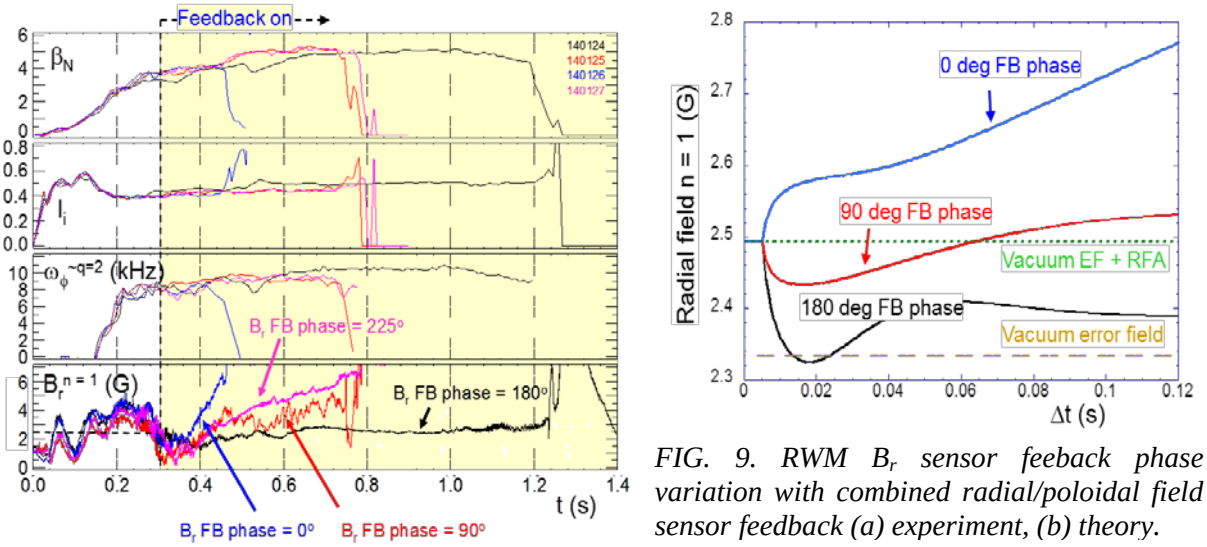

FIG. 9. RWM B_r sensor feeback phase variation with combined radial/poloidal field sensor feedback (a) experiment, (b) theory.

The second approach is a model-based RWM state space controller (RWMSC) [14] using a state derivative feedback algorithm [15], and incorporating currents due to the RWM unstable eigenfunction and those induced in nearby 3D conducting structure by the applied control field and plasma response. Testing this physics is especially important for ITER [16] and high neutron output devices where greater control coil shielding will be needed. The full 3D model with more than 3000 states, including the physical mode eigenfunction near marginal stability consistent with the kinetic RWM stability model, is reduced using a balancing transformation to less than 20 states. Open-loop comparisons between sensor measurements and the RWMSC model showed agreement with a sufficient number of states and improved agreement when details of the 3D wall model (including NBI ports) were added (Fig. 10). Using a number of states equal or greater than required by Hankel singular value analysis (7 here) provides sufficient 3D conducting structure current detail to match experimental sensors with greater fidelity during RWM activity. Control was demonstrated in long pulse, high β_N plasmas. Discharges were controlled which had n = 1 fields applied that would normally disrupt the plasma (Fig. 11). Plasmas limited only by coil heating constraints have exceeded β_N = 6.4, β_N/l_i = 13 using the RWMSC (Fig. 1).

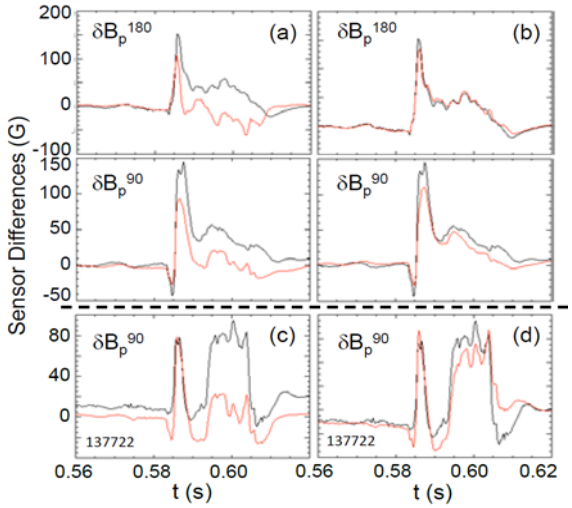

FIG. 10. Open-loop comparison of RWM sensor subset with RWMSC observer: a) 2 states, b) 7 states, c) without, and d) with the inclusion of the NBI port (7 states).

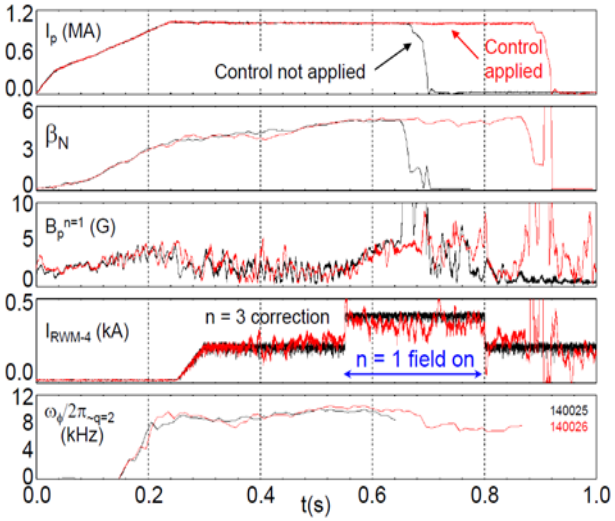

FIG. 11. High β_N NSTX plasma utilizing RWM state space control to survive an otherwise disruptive n = 1 perturbation.

6. Application of the kinetic RWM stabilization physics model to ITER

The kinetic RWM stabilization physics in the MISK and MARS-K (Dr. Y. Liu) codes were compared and benchmarked. The relevant frequencies and eigenfunctions now match between codes for both analytical Solov'ev and ITER equilibria. The numerical approach to the frequency resonance fraction energy integral taken in MISK [1] is equivalent to analytical limits computed in MARS-K. A comparison of the change in potential energy due to kinetic effects, δW_K, for $l = 0$ ions and electrons over a large range of $E\times B$ frequency normalized by Alfvén frequency, ω_A, for a Solov'ev equilibrium found good agreement between the codes (Fig. 12).

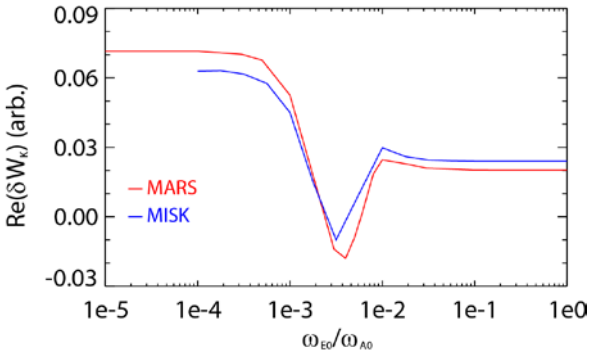

FIG. 12. Benchmarking comparison of δW_K for l=0 ions and electrons vs. scaled ω_E between MARS-K and MISK.

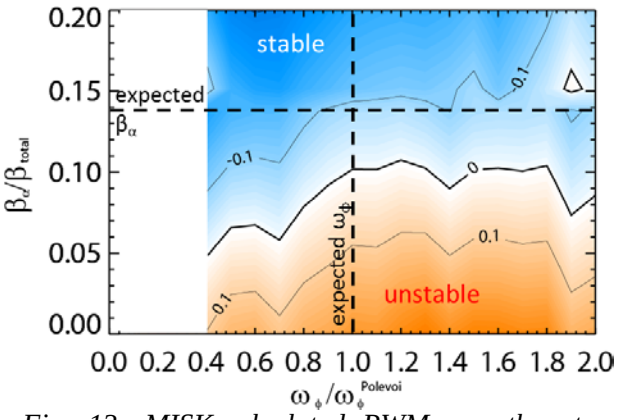

Fig. 13: MISK-calculated RWM growth rate contours vs. rotation and α particle β for ITER.

One result of these code improvements is application to ITER scenarios. ITER advanced scenario discharges were previously shown [2] to require alpha particles to maintain RWM stability due to the low expected toroidal rotation, a conclusion which still holds (Fig. 13).

Low rotation in ITER may not be entirely detrimental to RWM stability, however. Stability analysis has recently been performed on ITER advanced scenarios with internal transport barriers (ITBs) [17] that have strong internal gradients (see Fig. 14a). These can create a large ion diamagnetic frequency, ω_{*i}, which combined with relatively slow rotation can zero out the

$E\times B$ frequency, $\omega_E = \omega_\varphi - \omega_{*i}$ (Fig. 14b). The low ω_E effectively allows resonance between the mode and slowly precessing particles. Combined with the more "infernal" nature of the marginally stable eigenfunctions [17], strong kinetic stabilization can occur. Figure 15 shows that when the rotation is low enough in these ITB cases, kinetic resonance occurs and stabilization without alpha particles is possible. A potential issue with this approach is that ITBs can be transient, and their dynamics may result in RWM instability if profile dynamics move the plasma off-resonance. Active RWM control would then be needed during the period when the plasma profiles are away from stabilizing kinetic resonances.

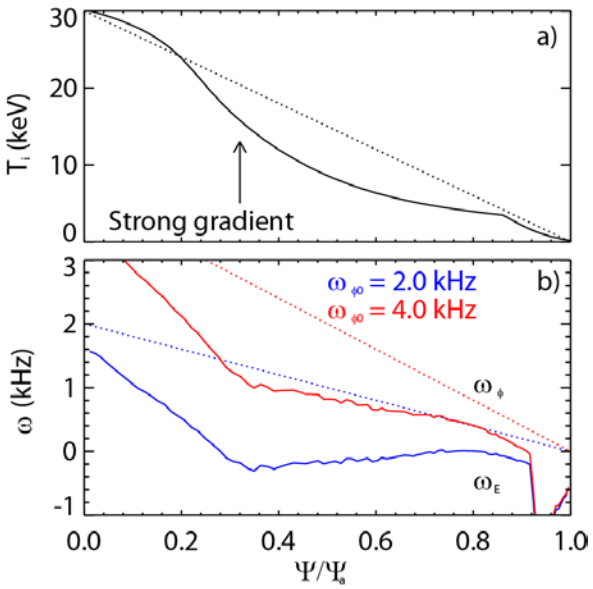

FIG. 14. a) T_i profile (with linear dashed line shown for reference), b) Linear toroidal rotation profiles, ω_φ, with 2 and 4 kHz core rotation, and the resulting ω_E profiles, all vs. ψ/ψ_a..

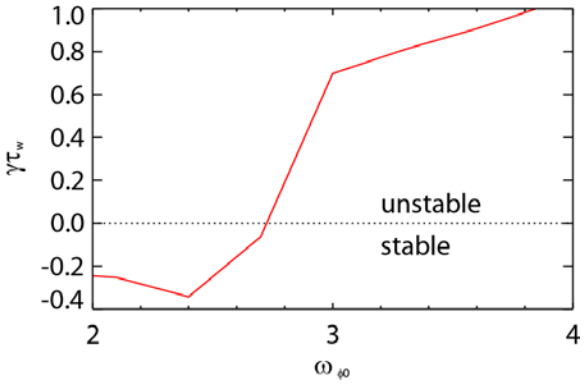

FIG. 15. Normalized growth rate, $\gamma\tau_w$, vs. linear rotation profiles with core value $\omega_{\varphi 0}$, for the ITER case with an ITB.

References

[1] BERKERY, J.W., SABBAGH, S.A., et al., Phys. Rev. Lett. **104** (2010) 035003.

[2] PENG, Y.K.-M, FOGARTY, P.J., et al., Plasma Phys. Control. Fusion **47** (2005) B263.

[3] BERKERY, J. W., SABBAGH, S.A., et al., Phys. Plasmas **17** (2010) 082504.

[4] SABBAGH, S.A., BELL, R.E., et al., Phys. Rev. Lett. **97** (2006) 045004.

[5] SABBAGH, S.A., BERKERY, J.W., et al., Nucl. Fusion **50** (2010) 025020.

[6] SABBAGH, S.A, SONTAG, A.C., BIALEK, J.M., et al., Nucl. Fusion **46** (2006) 635.

[7] MENARD, J.E., BROMBERG, L., BROWN, T., et al., Nucl. Fusion **51** (2011) 103014.

[8] REIMERDES, H., BERKERY, J.W., et al. Phys. Rev. Lett. **106** (2011) 215002.

[9] HANSON, J.M., TURCO, F., LANCTOT, M.J., et al., Proc. 24th Int. Conf. on Fusion Energy (San Diego, USA, 2012) (Vienna: IAEA) paper EX/P4-27.

[10] REIMERDES, H., CHU, M., et al., Phys. Rev. Lett. **93** (2004) 135002.

[11] ZHU, W., SABBAGH, S.A., BELL, R.E., et al. Phys. Rev. Lett. **96** (2006) 225002.

[12] BERKERY, J.W., SABBAGH, S.A., et al., Phys. Rev. Lett. **106** (2011) 075004.

[13] HU, B., BETTI, R., MANICKAM, J., Phys. Plasmas **12** (2005) 057301.

[14] SABBAGH, S.A., KATSURO-HOPKINS, O., et al., submitted to Phys. Rev. Lett.

[15] ABDELAZIZ, T.H.S.,VALASEK, M., Proc 16th IFAC World Congress, Prague (2005).

[16] KATSURO-HOPKINS, O., BIALEK, J.M., et al., Nucl. Fusion **47** (2007) 1157.

[17] POLI, F., KESSEL, C., CHANCE, M., et al., Nucl. Fusion **52** (2012) 063027.